INSTITUTE FOR ELECTRICAL ENERGY SYSTEMS
Chairman: Univ.-Prof. Dr.-Ing. Matthias Luther

Modelling of tranformers with on-load tap-changers (OLTC) in Python

MASTER THESIS

by

Maximilian Köhler, B. Eng.

March 31, 2025

[September 10, 2024 at 13:13 – preliminary version 0.1]

Maximilian Köhler: *Modelling of tranformers with on-load tap-changers (OLTC) in Python,*
Master Thesis, © March 2025

SUPERVISORS:
Ilya Burlakin, M. Sc.
Georg Kordowich, M. Sc.
Univ.-Prof. Dr.-Ing. Matthias Luther

LOCATION:
Erlangen

TIME FRAME:
01st October 2023 untill 31st March 2025

IMMATRICULATION NUMBER:
23176975

Abstract

The goal of this Master Thesis is the determination of the critical clearing time (CCT) of a synchronous generator (SG) in a simplified single machine infinite bus (SMIB) model. For this, a simple three-phase fault scenario is applied, and the generator swing equation is solved in the time domain with a Python-integrated solver. A function is implemented to calculate the CCT numerically, the result is compared to the analytical solution. Two additional fault scenarios are constructed, simulated and evaluated. These three cases illustrate the transient stability of a generator against an infinite bus bar (IBB), especially in a visual context with selected plots. The numerical algorithm shows satisfying results compared to the analytical. Limitations rely on the complexity of the considered electrical network, also in the additional fault scenarios, and the missing possible machine interaction. Further, the damping in the system is neglected completely, as well as any control unit of a SG (concrete the automatic voltage regulator (AVR), power system stabilizer (PSS) and governor (GOV)).

Kurzfassung

Das Ziel dieser Seminararbeit ist die Bestimmung der kritischen Fehlerklärungszeit am Beispiel eines Synchrongenerators in einem vereinfachten Einmaschinenmodell. Zu diesem Zweck wird ein einfacher dreiphasiger Kurzschluss angewandt, und die dynamische Bewegungsgleichung des Generators wird im Zeitbereich mit einem in Python integrierten Algorithmus gelöst. Eine Funktion wird implementiert, um die kritische Fehlerklärungszeit numerisch zu berechnen. Das Ergebnis wird zusätzlich mit der analytischen Lösung verglichen. Zwei weitere Fehlerszenarien werden erstellt, simuliert und ausgewertet. Diese drei Fälle veranschaulichen die transiente Stabilität eines Generators gegenüber einer starren und idealen Spannungsquelle mit Innenimpedanz, insbesondere in einem visuellen Kontext mit ausgewählten Diagrammen. Der numerische Algorithmus zeigt im Vergleich zum analytischen zufriedenstellende Ergebnisse. Limitationen zeigen sich in der Komplexität des betrachteten elektrischen Netzes, vor allem auch im Unterbrechungsszenario, und die fehlende mögliche Interaktion von multiplen Maschinen im Netz. Des weiteren wird die Dämpfung im System vollständig vernachlässigt, wie auch sämtliche Regler der Maschine (konkret die automatische Spannungsregelung (AVR), die Pendeldämpfung (PSS) und der Governor (GOV)).

Contents

Chapter 1

System stability in a changing grid

Our electrical energy system is drastically changing due to the shift towards renewable energy sources. This is not only changing the way to think about the energy supply itself, but also the challenges and requirements targeting the electrical energy system, its components and safety features. One aspect of understanding these challenges and ensuring a safe and robust operation is system stability assessments. One such analysis is the so-called transient stability assessment (TSA). [1]

Within this analysis, there are several indicators, methods, and perspectives. They will help understand the influences of power-electronics-dominated power systems, using technologies such as virtual inertia, FACTs and HVDC devices. This seminar and its resulting paper want to focus on synchronous generator (SG) and their key indicator in TSA: the critical clearing time (CCT). [2]–[6] The goal is the implementation of a CCT determing Python algorithm for a SMIB model. Therefore a handful of faults or interruption scenarios shall be simulated with the program. In combination with a few visualizations the concepts of transient stability assessment, and therefore determining the CCT and the critical power angle, are illustrated.

This leads to the following structure for the paper:

- **Chapter 2,**
  revising the fundamentals regarding SG, introducing the swing equation, introducing ways of stability analysis and presenting the SMIB model. Deriving the analytical solution to the CCT and giving a quick definition for system dynamics, its modeling and ODEs;
- **Chapter 3,**
  elaborating on the structure of the CCT assessment, giving (electrical)

pre-definitions and boundaries, and describing the implementation of the TDS and the EAC;

- **Chapter 4**,
  presenting the analytical and numerical results, showing a parameter influence on the CCT, discussing the results and marking the main limitations.

Chapter 2

Fundamentals

The following chapter wants to introduce basics about the SG, especially introducing the swing equation, giving an overview of the stability analysis including the SMIB model and the analytical calculation for the CCT. The sections 2.1, 2.2, 2.4 of the following chapter are recitations of various fundamental literature [3]–[9]. Paragraphs specifically from selected sources are marked as such.

2.1 Basics synchronous generators

Synchronous generators (SG) are used for electric power generation and thus connected to a mechanical power or toque input. For power plants most of the time this is a (steam) turbine. The main two types are the high-speed generator (often turbogenerator) and the low-speed generator (see Figure 2.1). The first one shows characteristics similar to those discussed in this paper. [4], [5]

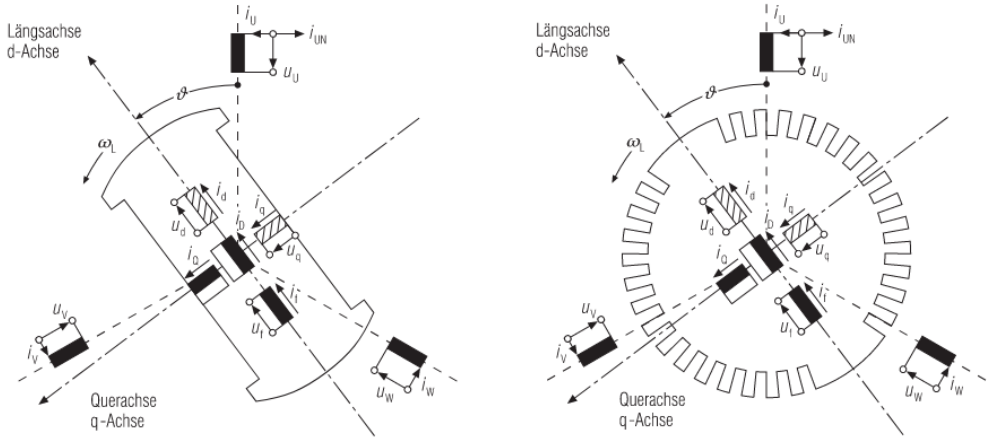

(a) low speed configuration **(b)** high speed configuration

Figure 2.1: Schematic view of types of synchronous generators (SGs); from [5]

Generators have a static part, the stator, and the moving rotor. The magnetic windings in the rotor are excited with an excitation voltage, the rotor is then turning inside the stator with the power of the turbine. In the stator, a three-phase current is injected and can be used for delivering electrical power to a connected grid. The whole principle is a balance between the electromagnetic forces, if the demanded power connected to the stator is too high, the rotor will slow down and vice versa. Usually, these generators have so-called damper windings, which dampens this dynamic and mechanical behavior. For this research paper, the damping effect is neglected. As well the regulation of the excitation voltage is seen as too complex for this paper. Further information is given in the sources [3]–[6]. Relevant for this paper is the so-called swing equation, which is describing the dynamic behavior of the SG.

The final swing equation system can be derived from the following two equations, which have to be solved in every time step to determine the pole angle δ and the rotor speed ω, respectively the rotor speed change from its base value $\Delta\omega$ [3], [4]:

$$\frac{d\delta}{dt} = \Delta\omega \tag{2.1}$$

$$\frac{d\Delta\omega}{dt} = \frac{1}{2 \cdot H_{\text{gen}}} \cdot (P_{\text{m}} - P_{\text{e}}) \tag{2.2}$$

where

δ	power angle (or power angle difference)
$\Delta\omega$	change of rotor angular speed
H_{gen}	inertia constant of the SG
P_{m}	mechanical power of the turbine
P_{e}	electrical power demanded and transferred out of the SG

2.2 System stability especially transient context

System stability can be divided into different areas, like in Figure 2.2 illustrated. For this paper relevant is the branch *Rotor angle stability - Transient stability*. The main drivers are electromechanical or electromagnetic phenomena, occurring and working rather fast in the sub-second to second range. Thermodynamic processes shall be neglected, so the governing equation is the swing equation from section 2.1.

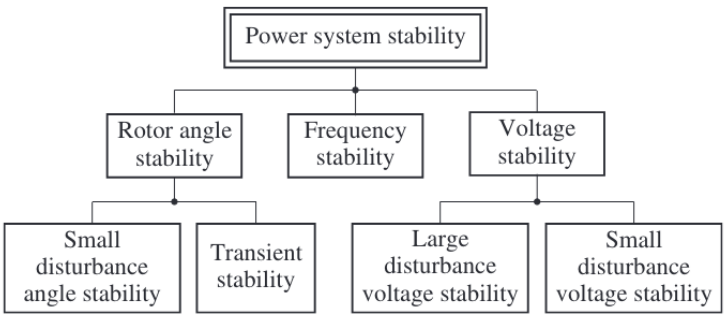

Figure 2.2: Classification of power system stability; three main indices with the (partly) time-related sub-division [4]

Transient stability assessment looks into fast disturbances like loss of generation, disconnecting of lines or busses, sudden faults and load changes, and the system's reaction to them. The main goal is to keep synchronism through a convergent behavior towards a new stable operation point. Concerning the limitations, that

1. the machine is operating under balanced three-phase positive-sequence conditions,
2. the machine excitation is constant,

3. the machine losses, saturation, and saliency are neglected,

a simplified single machine infinite bus (SMIB) model can be considered for transient stability assessment (see Figure 2.3). The IBB is operating with a constant voltage E_{ibb} and angle δ_{ibb}, typically set to $0°$. The real power flowing from the SG to the IBB is then expressed within the Equation 2.3 [3]–[5] and only dependent on the power angle δ, expressing the difference of the power angles when looking at two nodes. The reactance X_{res} expresses the simplified reactance from the respective circuit. E_{p} is describing the pole voltage of the SG.

$$P_{\text{e}} = \frac{E_{\text{p}} \cdot E_{\text{ibb}}}{X_{\text{res}}} \cdot sin(\delta) \tag{2.3}$$

The mechanical power of the turbine is assumed constant, due to the short occurrence of transient stability problems.

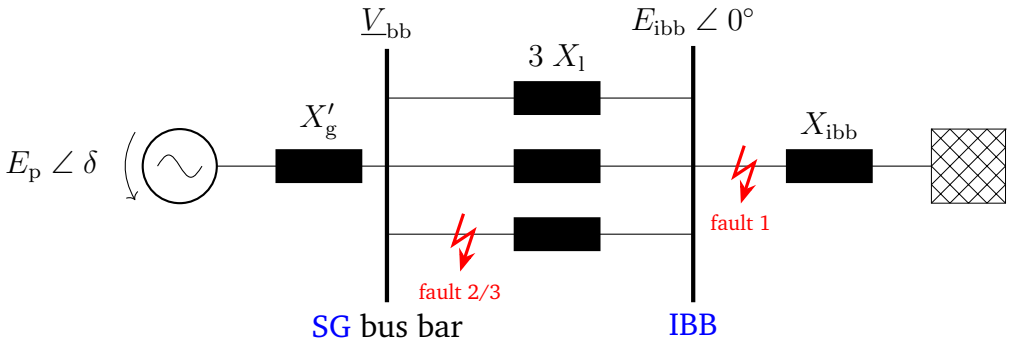

Figure 2.3: Representative circuit of a single machine infinite bus (SMIB) model with pole wheel voltage $E_{\text{p}} \angle \delta$ and infinite bus bar (IBB) voltage $E_{\text{ibb}} \angle 0°$; positions of considered faults 1 to 3 are marked with red lightning arrows

2.3 Analytical calculation of the critical clearing time

For the analytical solution of the swing equation and following the CCT, there is the need to find the critical

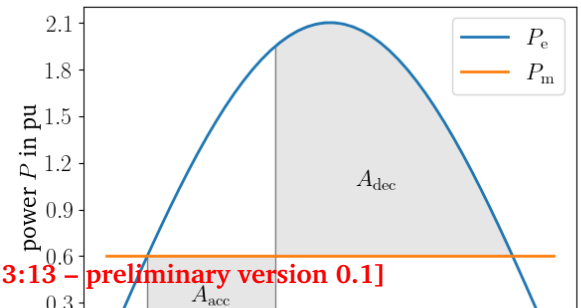

power angle δ_{cc} first. For this, the most common approach is the equal area criterion (EAC), considering that the amount of stored energy through acceleration (during the short circuit or failure) is equal to the released energy (decelerating the rotor) when synchronizing again. Both energy can be calculated through the area under the curve of the power difference $\Delta P = P_m - P_e$, while the accelerating area is between the first stable operating angle δ_0 and the clearing angle δ_c, the decelerating area between δ_c and the maximum dynamically stable angle δ_{max}. Figure 2.4 is illustrating this approach. Following this approach, a generalized expression is formed to

$$\int_{\delta_0}^{\delta_1} \Delta P \, d\delta = 0, \tag{2.4}$$

while the more expressive can be achieved through splitting up the integral borders and equalizing both areas:

$$\int_{\delta_0}^{\delta_c} (P_m - P_e) \, d\delta = \int_{\delta_c}^{\delta_{max}} (P_e - P_m) \, d\delta \tag{2.5}$$

With consideration of $\delta_{max} = \pi - \delta_0$, $P_{e,normal} = P_{max} \cdot sin(\delta_0)$, $P_{e,fault} = 0$, and some rearrangements, this leads to the final expression of the critical clearing angle:

$$\delta_{cc} = arccos\big[\, sin(\delta_0) \cdot (\pi - 2 \cdot \delta_0) - cos(\delta_0) \,\big] \tag{2.6}$$

The second step is the calculation of the CCT dependent on the critical clearing angle. Splitting the differentiated variables $d^2\delta$ and dt in the combined swing equation and integrating twice, leads to the equation

$$\delta = \frac{\omega \cdot \Delta P}{4 H_{gen}} \cdot t^2 + \delta_0.$$

Rearranging this gives an expression for calculating the critical clearing time t_{cc} (see Equation 2.7; similar to Oeding and Oswald [5]) for a full line fault

(meaning $P_{\mathrm{e,fault}} = 0$) at the bus bar. The derivation of this formula is added in **??**.

[MK1]: Vollständigen Rechenweg in den Anhang mit aufnehmen?

$$t_{\mathrm{cc}} = \sqrt{\frac{4H_{\mathrm{gen}} \cdot (\delta_{\mathrm{cc}} - \delta_0)}{\omega \cdot \Delta P}} \tag{2.7}$$

2.4 Numerical methods for system modeling

System dynamics enables the description, understanding, and discussion of complex problems in the context of system theory. They often can be described through a set of coupled ordinary differential equations (ODEs), most resoluted in time dimension [7]. ODEs can be solved through numerical integration with different methods. An easy and less complex method is Euler's method. It uses a linear extrapolation to calculate the function value at the next timestep, so following the iterable function [7]

$$f_{\mathrm{t+1}} = f_{\mathrm{t}} + \left(\frac{df}{dt}\right)_{\mathrm{t}} \cdot \Delta t, \tag{2.8}$$

with t being the discrete time step, Δt the time step size, and f an on t dependent function. Generally a system of second order ODEs can be rewritten as two first order equations. This often simplifies the calculation or the use of numerical methods. The presented swing equation of a SG in Equation 2.1 and Equation 2.2 has been split up by that principle. [7], [8], [10]

Python provides a handful of solvers, which can solve such first and second-order ODEs. As for this paper, the efficiency and run-time or error of the solver are not in the scope, simply the solver *odeint()* from the package *scipy* is used. The problem is thus explicitly solved.

Chapter 3

Numerical modeling

The following chapter will describe the implementation of Python Code for solving the derived ODE system (see section 2.1). For this, Python version 3.9 was used, in combination with the packages scipy, numpy, and matplotlib.[1] A similar model was implemented in Python by Kordowich [12]. This blog post provided inspiration and assistance for modeling in this paper.

3.1 Structure of the CCT assessment

The main interest of the algorithm is to determine the time until a system failure has to be resolved so that it can remain stable and synchronized. In general, an enough accurate and easy approach for a SMIB system is the EAC. For a more complex and coupled machine system, other approaches are more targeting. Some examples are given by Batchu, Raghuvamsi, and Teeparthi [13]. Further interest is to determine the associated critical clearing angle. This is the maximum possible power angle at the CCT, with which the fault can just be cleared into a stable system. At last one is interested in the time domain solution, just shortly before and after the CCT. This shall illustrate the convergent and divergent behavior of the power angle and therefore the rotor speed.

Figure 3.1 illustrates the structure of the numerical calculation. The single processes are further described in section 3.3 for the time resolution solving with *odeint()*, and section 3.4 for the function *determine_cct()*. The iterative solving of stable and unstable regime solutions neglects the fault start

[1] documentation and manual can be found on *https://scipy.org/* [11], similiar for *matplotlib*, and *numpy* packages

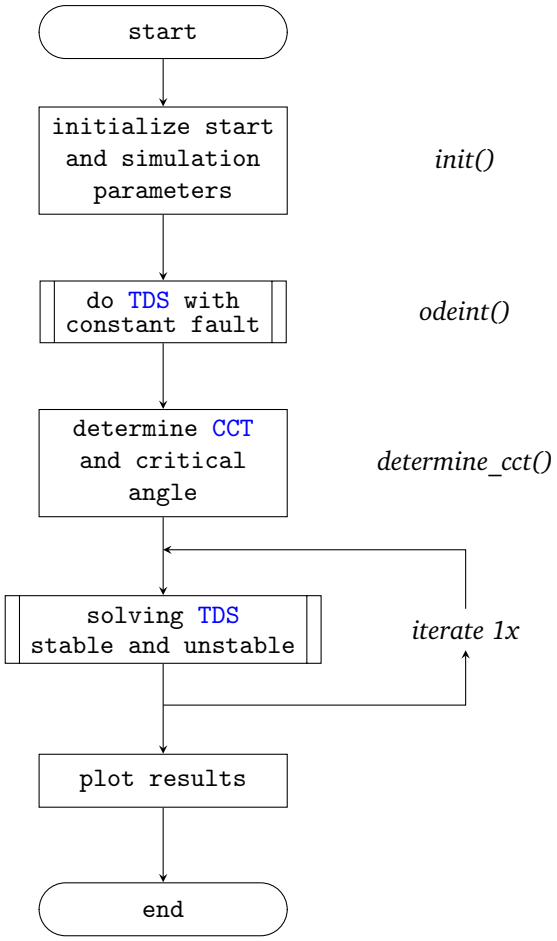

Figure 3.1: Program plan proposal for determining the critical clearing time (CCT) t_{cc}, critical power angle δ_{cc} and the time domain solution (TDS) of the single machine infinite bus (SMIB)-model; including the associated main function name

and ending as initial conditions, an identical procedure and using the same function set as the described TDS.

3.2 Electrical simplifications and scenario setting

3.2.1 Electric networks

The SMIB-model presented in Figure 2.3 has to be divided into the two states *during fault* and *steady state*, which can be used depending on a conditional statement, frame with time points. The most suitable description is a nodal admittance matrix.

Practically speaking from the swing equation (Equation 2.2), the real power flowing from the SG to the IBB is to be calculated. With the general equation for the real power [5] looking at the generator bus bar

$$P_\mathrm{e} = Re\{\underline{V} \cdot \underline{I}^*\},$$

and ohms law connected with the nodal admittance matrix for the voltage at the bus bar (see Equation 3.3 and 3.2; after [4], [5]), the only thing left for calculating the power is the injected current from the SG to the generator bus bar. The details we know about the SG help to describe it as a voltage source, but with a transformation, it can be used as a current source, delivering the injected current at the generator bus bar (see Equation 3.1; after [4]).

$$\underline{I}_\mathrm{inj} = \frac{\underline{E}}{jX} \tag{3.1}$$

$$\underline{V}_\mathrm{bb} = \underline{Y}_{11} \cdot \underline{I}_\mathrm{inj,gen} + \underline{Y}_{12} \cdot \underline{I}_\mathrm{inj,ibb} \tag{3.2}$$

$$\underline{I}_\mathrm{bb} = \frac{\underline{E}_\mathrm{gen} - \underline{V}_\mathrm{bb}}{jX} \tag{3.3}$$

where

$\underline{E}$	complex voltage
$\underline{I}_\mathrm{inj}$	current injection at the SG bus bar or the IBB
$\underline{I}_\mathrm{bb}$	current flowing from the SG bus bar
$\underline{V}_\mathrm{bb}$	voltage at the bus bar
$\underline{Y}$	admittance

3.2.2 Simulation cases and boundaries

The boundaries of the single cases, which are simulated, are given with a Python dictionary. Therefore the values of the variables have to be predefined and documented. Considering fault cases, there are three differences in the interest:

1. A three-phase short circuit at the IBB and disconnection of the complete electrical power. The CCT of the fault has to be determined, a TDS with fault clearing shortly before and after the critical clearing is carried out and displayed as *stable* and *unstable*;

2. A partial line fault at the SG bus bar, meaning just a defined percentage of the electrical power is disconnected. Further evaluation is carried out like in scenario 1;

3. A partial line cutting, meaning just a defined percentage of the electrical power is disconnected. But with consideration, that the fault condition is stable at a new operation point. This operating point is calculated in the time domain.

Further of interest is a parameter variation of both influences H_{gen} and ΔP. This last parameter is not meant to describe the absolute power difference, which is inserted into the swing equation, but more the power difference relative to the maximum electrical power output of the generator. Due to the relation between the maximum power output and the disconnected electrical power in the acceleration and deceleration of the rotor, it seems more significant to use this as a relative parameter. The CCT in dependency of these two influences shall be elaborated.

3.2.3 Initial value calculation

For the setting of starting values, the per-unit system is preferred. Because of the relative nature of this unit, it acts as a generalization and can be applied to concrete examples with known nominal sizes. Generally speaking, $P_{\text{e,max}}$, $P_{\text{e}} = P_{\text{mech}}$, E_{ibb}, E_{gen}, δ_{ibb} and δ_{gen} are needed to be predefined for the simulation.

As the point of interest in most calculations, the voltage at the IBB is set to $E_{\text{ibb}} = 1$ p.u.. Most of the now presented equations refer to power angle differences. For a simplified calculation, it is convenient to set the power angle of the IBB to $\delta_{\text{ibb}} = 0°$, thus all the power angle and angle developments dependent on the time are solely related to the absolute power angle of the generator. The maximum electrical power of the generator is arbitrarily set to $P_{\text{e,max}} = 1.2$ p.u., and the real power extracted from the generator into the grid node is set to $P_{\text{e}} = P_{\text{m}} = 0.9$ p.u.. With these predefinitions and both following equations, we can calculate the remaining two values.

$$E_{\text{gen}} = \frac{P_{\text{e,max}} \cdot X}{E_{\text{ibb}} \cdot sin(90°)} \approx 1.14 \text{ p.u.}$$

$$\delta_{\text{gen}} = arcsin\left(\frac{P_{\text{e}} \cdot X}{E_{\text{ibb}} \cdot E_{\text{gen}}}\right) \approx 48.6°$$

The reactances for the different fault scenarios can be derived from the electrical network and the scenario setting. Therefore for each failure mode, a new nodal admittance matrix is calculated and handed over in addition to the steady initial state. The last one is constituted by the reactance of the generator, the line(s), and the IBB. For fault one the additional fault reactance is getting very high in addition to the generator, thus it can be neglected. Fault two, considering just a partial line tripping and thus removal of one of the three lines, is increasing the contribution from the lines to $\frac{3}{2}$ of its initial value. This means instead of $\frac{1}{3} \cdot X_\mathrm{l}$ the overall line reactance is $\frac{1}{2} \cdot X_\mathrm{l}$. The other contributions stay consistent. The mechanical power is higher at $1.0\ \mathrm{p.u.}$ with a power angle of $56.4°$. For fault scenario three the initial values are the same as in fault two, although the interrupting scenario is not cleared. The initial electrical power is lowered to $0.7\ \mathrm{p.u.}$ and thus the initial power angle of the generator is set to $35.7°$. A compromised overview of the initial values and the values in the fault cases is given in section A.1.

3.3 Implementation of the time domain solution

The TDS shall be solved with a python-integrated solver, due to the fact that numerical solving methods are not the scope of this paper. The solver *odeint()* from the *scipy*-package is therefore used as a preferred algorithm. This requires a time array with all the timesteps of interest and a differential function, which is solved through every time step. Due to the second-order nature of the swing equation and just the possibility of solving first-order ones, the equation has to be split up into two first-order equations and solved simultaneously. This can be realized by using a solution array instead of a variable.

Looking deeper into the swing equation, both the demanded electrical power from the grid or connected network and the mechanical power put into the rotor of the SG from the steam turbine have to be calculated at each time step. While the mechanical power is a bit easier to calculate, the electrical power is more complex. To get a good representation, the algebraic equations describing the connected network (see subsection 3.2.1), have to be solved at every time step as well. For this a dedicated function *algebraic()* is included.

3.4 Implementation of the equal area criterion

The equal area criterion (EAC) is computed as the name states. It is comparing the accelerated area with the decelerable area, and therefore comparing the stored to the braking (or re-synchronizing) energy. The main function *deteming_cct()* is differentiating between clearing and non-clearing mode. The first one is taking the pre-fault status of the connected network also as the post-fault condition, thus calculating the clearing time and angle the generator and the network can remain in the fault state. The non-clearing mode takes the fault condition as the post-fault condition and calculates a new stable power angle convergent.

The main thought is iterating through the TDS at each time step, looking if enough braking reserve is left and saving the current time and angle as a solution. If the loop continues, the solution is overwritten. As pre-set the solution is negative. This enables a quick understanding of simulation faults or a general unstable initial condition set.

As a helping function *stability_eac()* allows a simple check in the loop. It calculates the currently passed acceleration area, and until the maximum dynamically stable power angle $\delta_{\max} = \pi - \delta_0$ possible decelerating area, it can compare and state stability or instability at the current time point.

Another possible way would be to check the stability first under the $P - \delta$-curve, gathering the critical angle. After that, a simple run through the TDS can deliver the searched CCT. Within this approach, the angle spectrum has to be searched in addition to the TDS. This doubled vector searching seemed an easy improvement in comparison to the previous method and was therefore neglected.

Chapter 4

Results

4.1 Analytical results

The analytical calculation follows the equations from section 2.3. For fault one the simplified ones could be used, the more complex and advanced ones are needed for fault case two. Therefore the base values for the first two input scenarios are used according to the numerical simulation. For the third one, no CCT is calculatable, due to the stable nature of the fault scenario. The results of this calculation are shown in Table 4.1.

Table 4.1: Analytical results for the two clearing fault-scenarios; considering δ_{cc} and t_{cc}

scenario	δ_{cc}	t_{cc}
fault 1	65.01°	0.116 s
fault 2	93.99°	0.595 s

MK2]: Was
t mit nicht
ollständigen
ehlern?
leichungen
r analytical
eschreiben
chts...
erte für
ult 2 de-
entsprechend
gentlich
lsch und
hen auch
lsch aus.

4.2 Numerical results

Table 4.2 is summarizing the results for the CCT-calculation of the different set scenarios in section 3.2. Similar to the analytical results section before, the third fault can not be displayed in the context of the first

Table 4.2: Results (CCT and δ_{cc}) for numerical solving the faults 1, 2, and 3

scenario	δ_{cc}	t_{cc}
fault 1	65.9°	0.119 s
fault 2	89.3°	0.34 s

two clearing ones. The maximum reached power angle for fault three is $70.5°$, while the new stable power angle is around $52.1°$. At first, the system oscillates around this new angle, until the damping factor results in a new stable and steady operation point.

4.2.1 Simulated faults

Looking deeper into the numerical results is possible by plotting the development of the power angle over time. In addition to that the used energies or respective areas in the P-δ-curves. Figure 4.1 is looking deeper into the non-clearing fault three. Because of spacial reasons, the complete plot sets for all faults are included in the section A.2, section A.3 and section A.4.

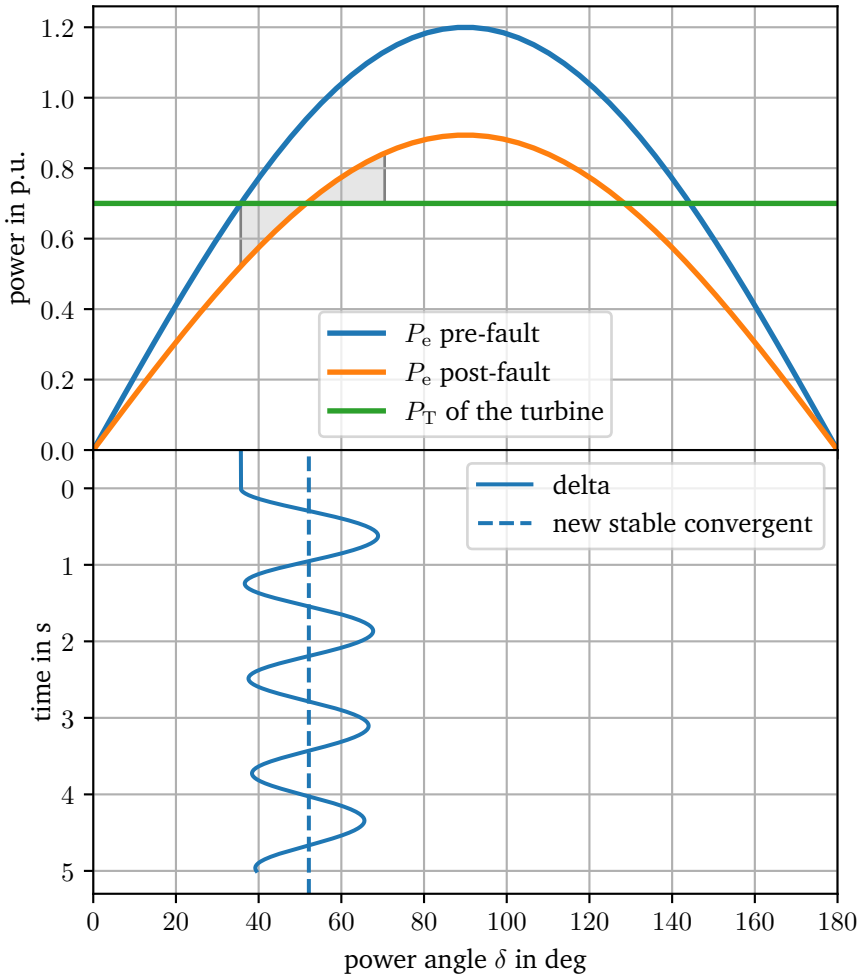

Figure 4.1: Power angle plot of fault 3 in time and power domain; grey areas illustrate the used area under the curve for storing and releasing kinetic energy in/out of the rotor

Both partial sinus functions represent the electrical power demanded from the electrically connected network. During the fault, in this case, post-fault as well is lower in the peak thus giving another intersection point with the straight horizontal mechanical power from the turbine. The new stable convergent is falling together with this intersection point. The used area reaches from the starting power angle over the post-fault intersection point to the maximum swept power angle in the time resolution. In this case, the fault is starting to occur at the time point 0 s.

For faults one and two the whole area until the maximum dynamic stable operation point, the second intersection point with the pre-fault partial-

sinoidal wave, is used. Therefore the critical angle is not at the intersection with the during-fault electrical power curve. In the unstable scenario, clearing the fault just a few time steps after the CCT leads to a divergent power angle. Clearing just in time shows a stable, oscillating behavior while resulting in a maximum overswing in the region of the maximum dynamic stable power angle. This behavior can be seen in fault one as well as in fault two, while in fault one the static stable angle cannot be reached, and in fault two it is even overstepped.

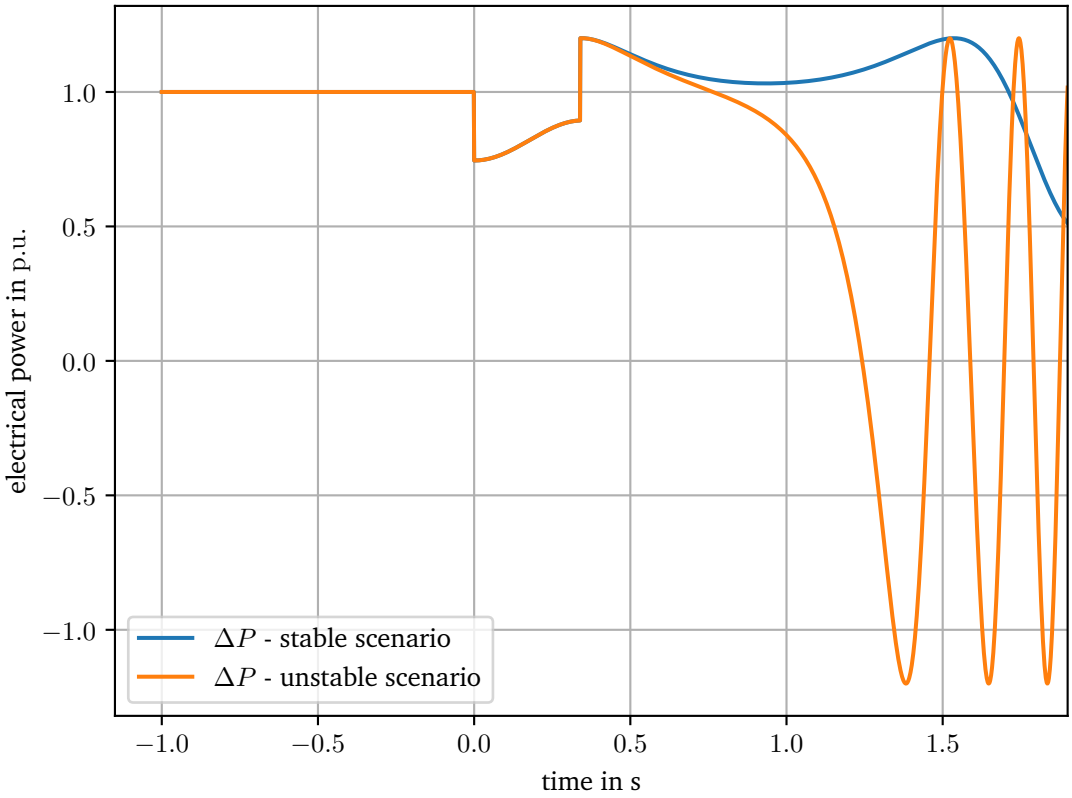

Figure 4.2: Power difference behavior over time for fault 2; stable operation mode in negative time regime, the fault is occurring between 0 s and 0.394 s

Plotting the electrical extracted power P_e of fault two against the time the power swings in the stable and the unstable case are visible. While stable operation before the fault occurs, it is on one continuous value. As soon as the line is shorted, the electrical power sinks suddenly down, with the fault duration it is getting bigger again. With clearing the fault another jump is happening to a greater power value than initially in stable operation, followed by an oscillation of the power. While in the stable case, the swings have a

bigger oscillation period and do not cross into the negative real power regime, the unstable case swings relatively fast and shows extreme values ranging far into the negative regime. A similar result can be seen within the fault one. One exception: the electrical power during the fault is zero because of the missing fault reactance and thus, no real power can be extracted from the generator. While fault three is present, a first jump with the fault occurrence is observable. After that, the real power swings around the before stable power output. As in Figure 4.1 illustrated, a new stable operation point is given by the new intersection of the power curves with a new stable power angle.

4.2.2 Using algebraic calculations or non-algebraic calculations

Using the non-algebraic approach in calculating, the TDS seems to have a similar result. A slight difference can be spotted in the swings of the power angle for the duration of a swing period. The time-dependent power angle and electrical power behavior are observable in section A.5.

If this is just an alternative for the given simple use-case of a SMIB model, or if it is usable in other scenarios as well, can not be stated at this point. Where applicable, there may maybe other (electrical) pre-simulation reduction methods necessary.

4.2.3 Parameter influence analysis

Other variables changing the CCT of a generator are the power difference ΔP and the generator inertia constant H_{gen} (see Equation 2.2). The resulting CCT while varying this parameter in the ranges

$$H_{\text{gen}} = [0,\ 12]\ \text{s},\ \text{and}$$
$$\Delta P = [25,\ 91.7]\ \%$$

is shown in Figure 4.3.

Good visible is the similar progression of the CCT. With increasing H_{gen} the CCT is getting higher as well. The lower the electrical extracted power is

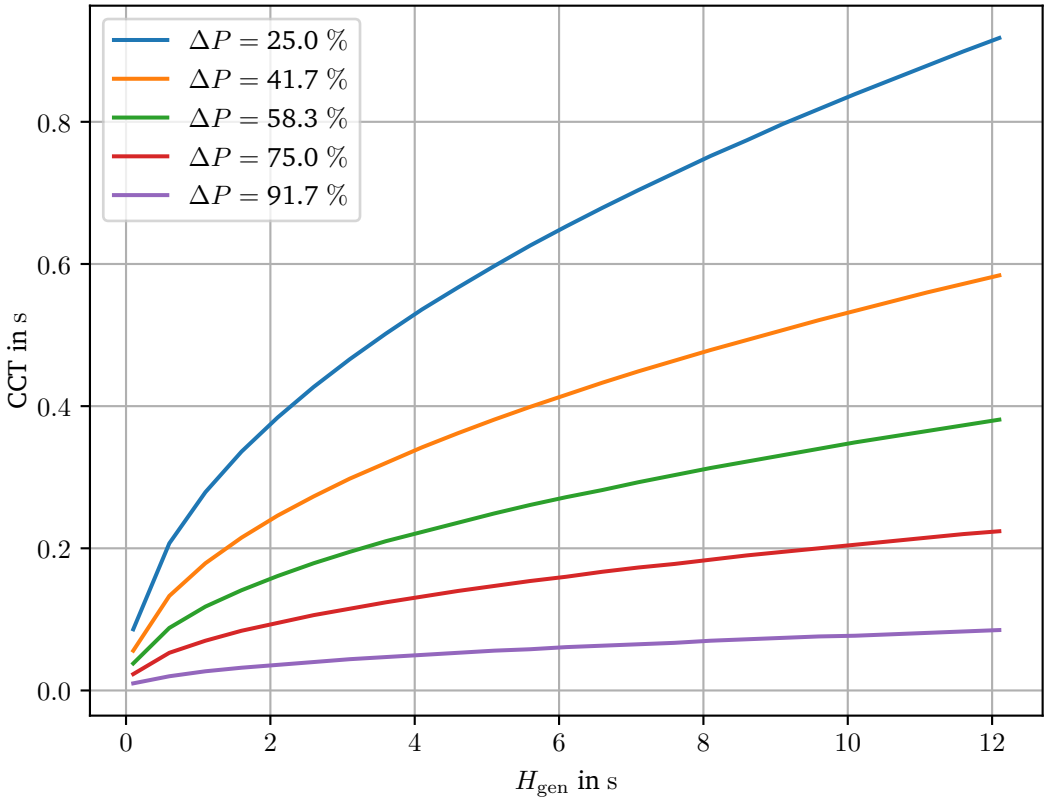

Figure 4.3: Influence of varying the parameters power difference ΔP and generator inertia constant H_{gen} on the critical clearing time (CCT)

to the maximum electrical power, the bigger the CCT is. This effect is also non-linear and increases with a lowering ΔP.

4.3 Discussion

The determination of the CCT with the EAC gives results with an error of $2.5\ \%$ compared to the analytical solution. The critical power angle shows an error of $1.7\ \%$. For this calculation, only fault case one is considered. The analytical solution of fault two seems not representative, due to the calculation with $P_{\text{e,fault}} = 0$, giving a different area to accelerate. The plots show expected characteristics, such as the stable power angle in the beginning, equal areas regarding the maximum reached power angles in the stable case or a slightly higher critical power angle in the unstable case. Additionally, extreme or turning points are conclusive within the different representations and could be expected in the simulated way.

The difference between using algebraic equations for describing the power flow from the SG bus to the IBB and the simplified calculation of the real power equation (Equation 2.3) is neglectable. This shows, that within a two-point system, like the SMIB, with simple occuring events, using only one equation with calculating a X_{res} would be satisfying. Possibly this would help reduce code size, running time and needed storage.

The influences of the inertia constant H_{gen} and the relative power loss were suspected like the simulation result. Looking at Equation 2.7 the dependencies

$$t_{\text{cc}} \propto \sqrt{H_{\text{gen}}}, \text{ and}$$

$$t_{\text{cc}} \propto \sqrt{\frac{1}{\Delta P}},$$

this simulation shows identical behavior. The simulation only expands the qualitative relationship into a quantitative one, using numerical values from the considered cases.

4.4 Limitations

After presenting and discussing the results of this paper, one major aspect left is the aspects not covered by the model. Generally speaking, an optimization of the algorithm with regards to storage, and computing power requirements, as well as running time, are not considered at all.

MK3]: Da abs auch och einen eiteren enerellen unkt...

Regarding the possible three responses to a transient disturbance, stability, first-swing stability and metastable, only the first two ones could be displayed. For the metastable case[2], an additional small-signal instability in a resulting transient stable clearing would have been needed to model. [3]

In the model, there was no single damping mechanism considered. The damping in the machine itself, or from other machines or connected loads would require additional modeling and equations to solve. This missing would for example explain the long oscillation duration around the new stable convergent power angle in fault case three.

Another point is the largely simplified SMIB model. Although it is simple to set up and already powerful in its results, it can not model machine interactions

[2] one or some stable swings before an unstable behavior is occuring

or more than two busses, therefore various other fault cases as well. For a TSA of a machine group, other algorithms as the simplified EAC would have been needed as well [13]. Determining transient stability is thus possible with other methods, not only looking into areas of the P-δ-curves but also considering the current angle, current power flow status of the SG or others. The presented method is however easy to apply, good in the result and ideal for an initial understanding.

Chapter 5

Summary and outlook

In conclusion a single machine infinite bus (SMIB) model was implemented into Python, using the swing equation of a synchronous generator (SG) and the algebraic equation set of the electric network. A function for determining the critical clearing time (CCT) was delivering satisfying results in comparison to the analytical solution. Three faults or interrupting events were defined, implemented and simulated, especially regarding the CCT. The simulation results were plotted in an overlay of P-δ-curves with marked equal accelerating and decelerating areas, and the associated time domain solution (TDS). This was done for just stable and just unstable clearing of the fault. In addition, the electrical injected power from the SG into the infinite bus bar (IBB) for stable and non-stable fault cases was illustrated on a time scale basis.

This paper shows on one side the simple indicator CCT for a transient stable operation of a SG. On the other hand, with all the limitations and outlooks, the topic of determining stability and therefore the CCT can become very complex when considering heavily interconnected electrical networks, machine interactions, or non-trivial interruption events. The importance of this analysis, especially for an electrical power system changing towards newer and faster-responding technologies meeting expectations and challenges of renewable energy sources (like Gao, Du, and Wang [14]), cannot be denied.

Acronyms

CCT	critical clearing time
EAC	equal area criterion
IBB	infinite bus bar
ODE	ordinary differential equation
SG	synchronous generator
SMIB	single machine infinite bus
TDS	time domain solution
TSA	transient stability assessment

Symbols

δ	$^\circ$ / deg	power angle (or power angle difference)
$\Delta\omega$	$\frac{1}{\mathrm{s}}$	change of rotor angular speed
A	-	acceleration or deceleration area
E	V	voltage of SG or IBB
H_{gen}	s	inertia constant of a synchronous generator (SG)
I	A	current
P	W	Power; electrical or mechanical
V	V	voltage
X	Ω	reactance
Y	$\frac{1}{\Omega}$ / S	admittance

In the simulations and calculations the per unit system is preferred, thus using all values as per reference unit ($\mathrm{p.u.}$). Where necessary indices are used to differentiate between similar symbols with different values.

List of Figures

List of Tables

Bibliography

[1] "Perspektiven der elektrischen Energieübertragung in Deutschland", VDE Verband der Elektrotechnik Elektronik Informationstechnik e.V., Ed., Frankfurt am Main, Apr. 2019.

[2] J. D. Glover, T. J. Overbye, and M. S. Sarma, "Power system analysis & design", Boston, MA, 2017.

[3] P. S. Kundur and O. P. Malik, *Power System Stability and Control*, Second edition. New York Chicago San Francisco Athens London Madrid Mexico City Milan New Delhi Singapore Sydney Toronto: McGraw Hill, 2022, 948 pp., ISBN: 978-1-260-47354-4.

[4] J. Machowski, Z. Lubosny, J. W. Bialek, and J. R. Bumby, *Power System Dynamics: Stability and Control*, Third edition. Hoboken, NJ, USA: John Wiley, 2020, 1 p., ISBN: 978-1-119-52636-0 978-1-119-52638-4.

[5] D. Oeding and B. R. Oswald, *Elektrische Kraftwerke und Netze*, 8. Auflage. Berlin [Heidelberg]: Springer Vieweg, 2016, 1107 pp., ISBN: 978-3-662-52702-3. DOI: 10.1007/978-3-662-52703-0.

[6] A. J. Schwab, *Elektroenergiesysteme: smarte Stromversorgung im Zeitalter der Energiewende*, 7. Auflage. Berlin [Heidelberg]: Springer Vieweg, 2022, 871 pp., ISBN: 978-3-662-64773-8.

[7] S. Georgiev and I. M. Erhan, *Numerical Analysis on Time Scales* (De Gruyter Graduate). Berlin: De Gruyter, 2022, 382 pp., ISBN: 978-3-11-078725-2.

[8] W. Miles, *Numerical Methods with Python: For the Sciences* (De Gruyter Textbook). Berlin ; Boston: De Gruyter, 2023, 314 pp., ISBN: 978-3-11-077645-4.

[9] H. P. Langtangen, *A Primer on Scientific Programming with Python* (Texts in Computational Science and Engineering 6), 5th edition. New York, NY: Springer Berlin Heidelberg, 2016, ISBN: 978-3-662-49886-6.

[10] D. F. Griffiths and D. J. Higham, *Numerical Methods for Ordinary Differential Equations: Initial Value Problems* (Springer Undergraduate Mathematics Series). London: Springer, 2010, 271 pp., ISBN: 978-0-85729-147-9.

[11] P. Virtanen, R. Gommers, T. E. Oliphant, *et al.*, "SciPy 1.0: Fundamental algorithms for scientific computing in Python", *Nature Methods*, vol. 17, no. 3, pp. 261–272, Mar. 2, 2020, ISSN: 1548-7091, 1548-7105. DOI: 10.1038/s41592-019-0686-2. [Online]. Available: https://www.nature.com/articles/s41592-019-0686-2 (visited on 01/13/2024).

[12] G. Kordowich. "Watts Up with Dynamic Power System Simulations", medium.com. (2023), [Online]. Available: https://medium.com/@georg.kordowich/watts-up-with-dynamic-power-system-simulations-c0f16fc99769.

[13] S. Batchu, Y. Raghuvamsi, and K. Teeparthi, "A Comparative Study on Equal Area Criterion Based Methods for Transient Stability Assessment in Power Systems", in *2022 22nd National Power Systems Conference (NPSC)*, New Delhi, India: IEEE, Dec. 17, 2022, pp. 124–129, ISBN: 978-1-66546-202-0. DOI: 10.1109/NPSC57038.2022.10069303. [Online]. Available: https://ieeexplore.ieee.org/document/10069303/ (visited on 12/14/2023).

[14] Z. Gao, W. Du, and H. Wang, "Transient stability analysis of a grid-connected type-4 wind turbine with grid-forming control during the fault", *International Journal of Electrical Power & Energy Systems*, vol. 155, p. 109 514, Jan. 2024, ISSN: 01420615. DOI: 10.1016/j.ijepes.2023.109514. [Online]. Available: https://linkinghub.elsevier.com/retrieve/pii/S0142061523005719 (visited on 12/15/2023).

Author's declaration

I certify that I have prepared this Master Thesis without outside help and without using sources other than those specified and that the thesis has not been submitted in the same or a similar form to any other examination authority and has not been accepted by them as part of an examination. All statements that have been copied verbatim or in spirit are marked as such.

Erlangen, September 10, 2024

_____

Maximilian Köhler, B. Eng.

Note:

For reasons of readability, the generic masculine is primarily used in this Master Thesis. Female and other gender identities are explicitly included where this is necessary for the statement.

Appendix

Appendix A

Graphics and tables

A.1 Initial values

	fault 1	fault 2	fault 3
$P_{\text{e, max}}$	1.2 p.u.		
P_{mech}	0.9 p.u.	1.0 p.u.	0.7 p.u.
E_{ibb}	1 p.u.		
E_{gen}	1.14 p.u.		
δ_{ibb}	48.6 deg	56.4 deg	35.7 deg
δ_{gen}	0 deg		
$Y_{\text{bus, init}}$	$\begin{bmatrix} -\frac{1j}{X_{\text{gen}}} - \frac{3j}{X_{\text{line}}} & \frac{3j}{X_{\text{line}}} \\ \frac{3j}{X_{\text{line}}} & -\frac{3j}{X_{\text{line}}} - \frac{1j}{X_{\text{ibb}}} \end{bmatrix}$		
$Y_{\text{bus, fault}}$	$\begin{bmatrix} -\frac{1j}{X_{\text{gen}}} - \frac{3j}{X_{\text{line}}} + 10^6 & \frac{3j}{X_{\text{line}}} \\ \frac{3j}{X_{\text{line}}} & -\frac{3j}{X_{\text{line}}} - \frac{1j}{X_{\text{ibb}}} \end{bmatrix}$	$\begin{bmatrix} -\frac{1j}{X_{\text{gen}}} - \frac{2j}{X_{\text{line}}} & \frac{2j}{X_{\text{line}}} \\ \frac{2j}{X_{\text{line}}} & -\frac{2j}{X_{\text{line}}} - \frac{1j}{X_{\text{ibb}}} \end{bmatrix}$	
t_{start}	-1 s		
t_{end}	2 s		5 s
t_{step}	0.001 s		
$t_{\text{fault, start}}$	0 s		

For the modules *parameter_comparison.py* and *comparison_alg-vs-nonalg.py* the initial values from fault one are used, besides the described variations.

X_{line}	1.95 p.u.
X_{gen}	0.2 p.u.
X_{ibb}	0.1 p.u.

H_{gen}	3.3 s
f_{n}	50 $\frac{1}{\text{s}}$
ω	0

d

A.2 Fault 1

Stable scenario - fault 1

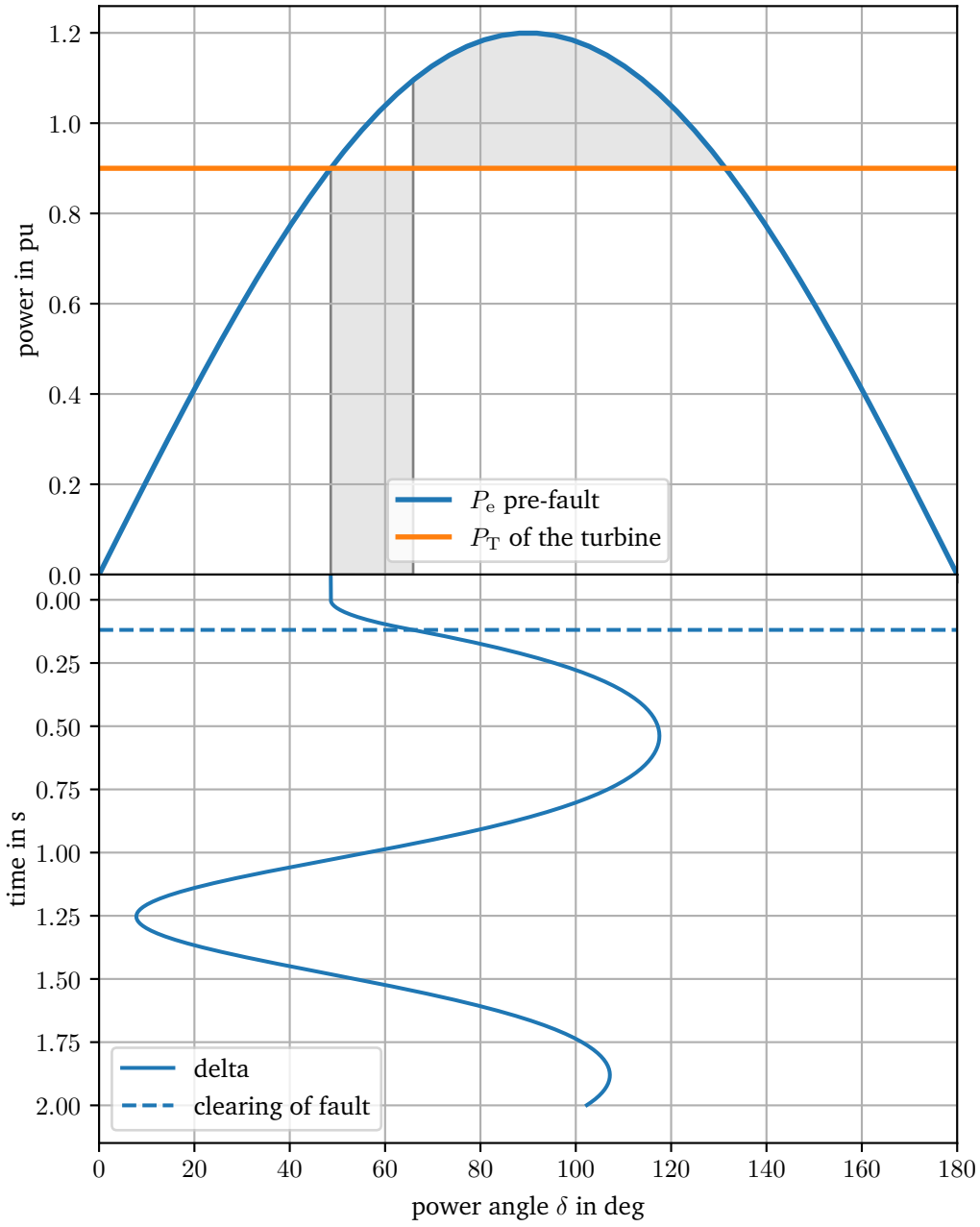

e

Unstable scenario - fault 1

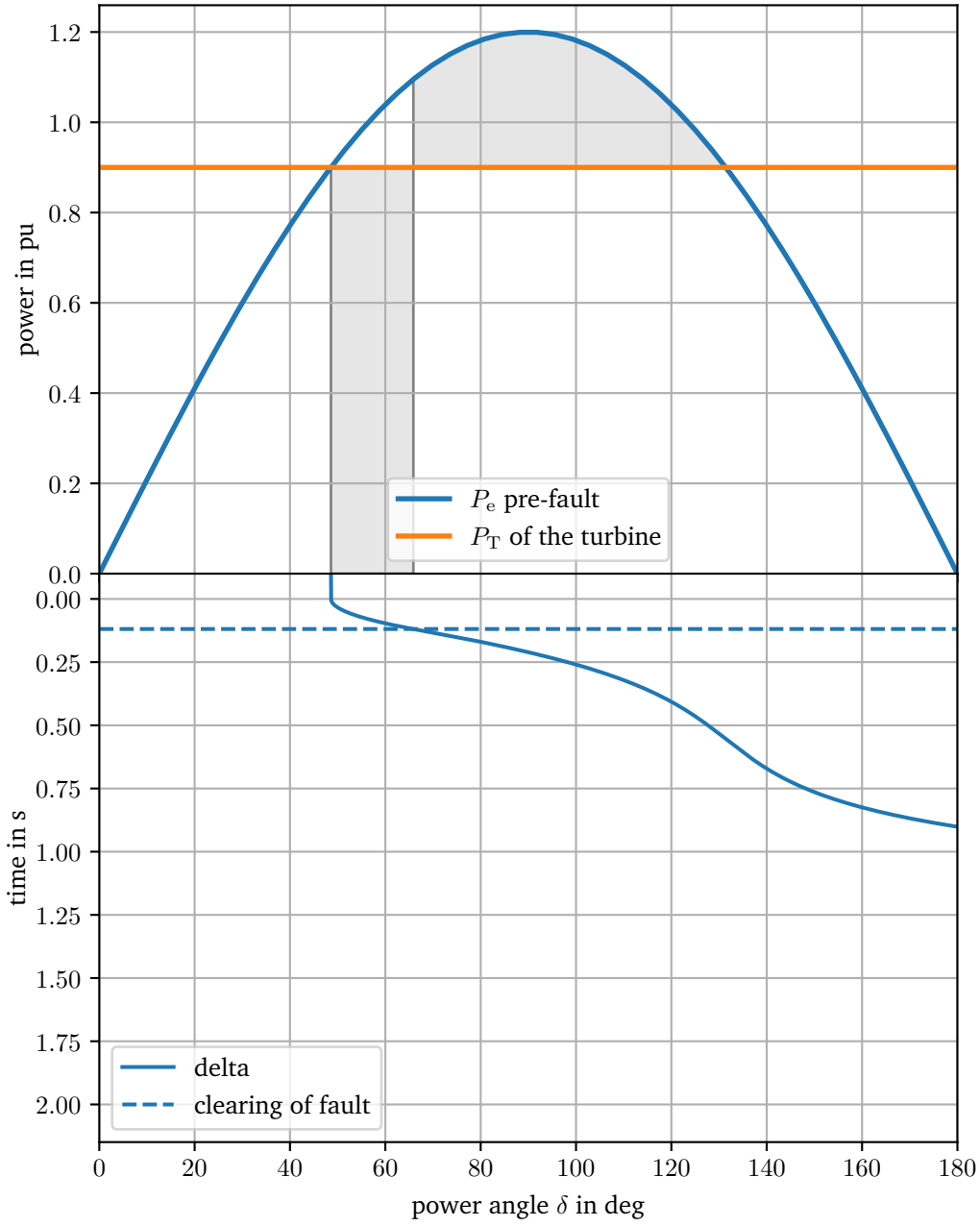

f

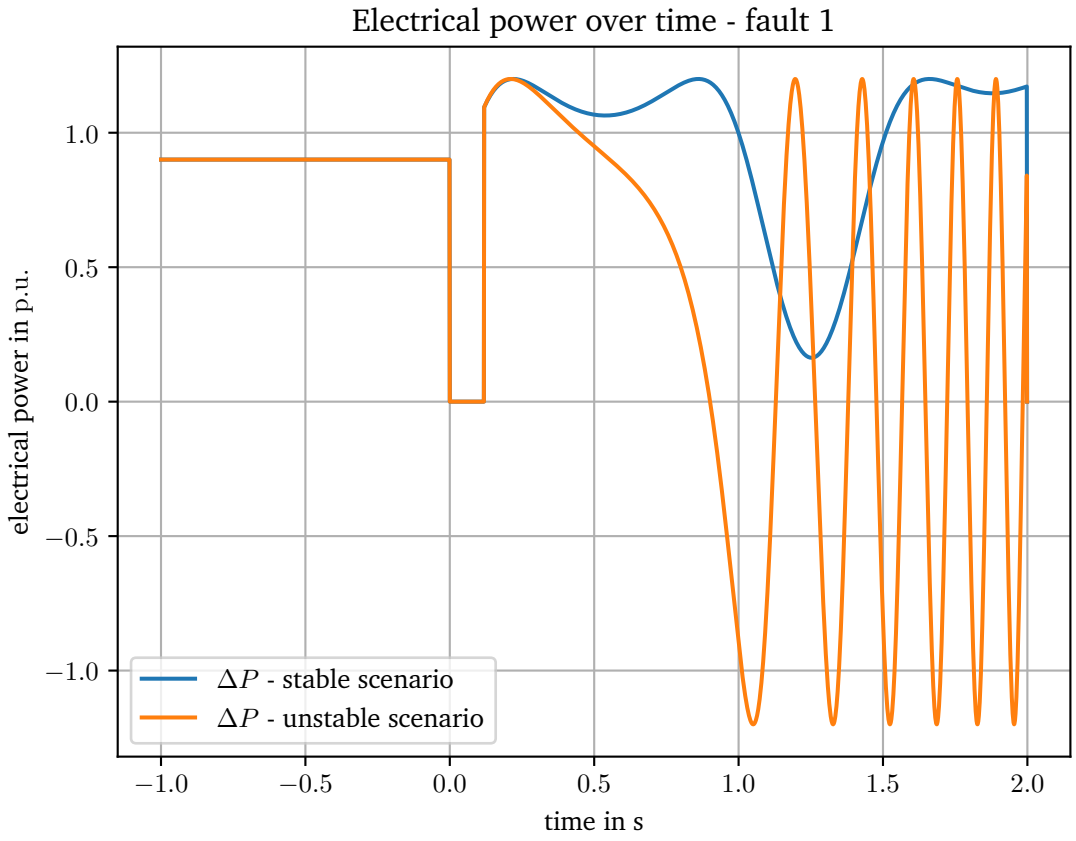
Electrical power over time - fault 1
electrical power in p.u.
time in s
1.0
0.5
0.0
−0.5
−1.0
−1.0
−0.5
0.0
0.5
1.0
1.5
2.0
ΔP - stable scenario
ΔP - unstable scenario

A.3 Fault 2

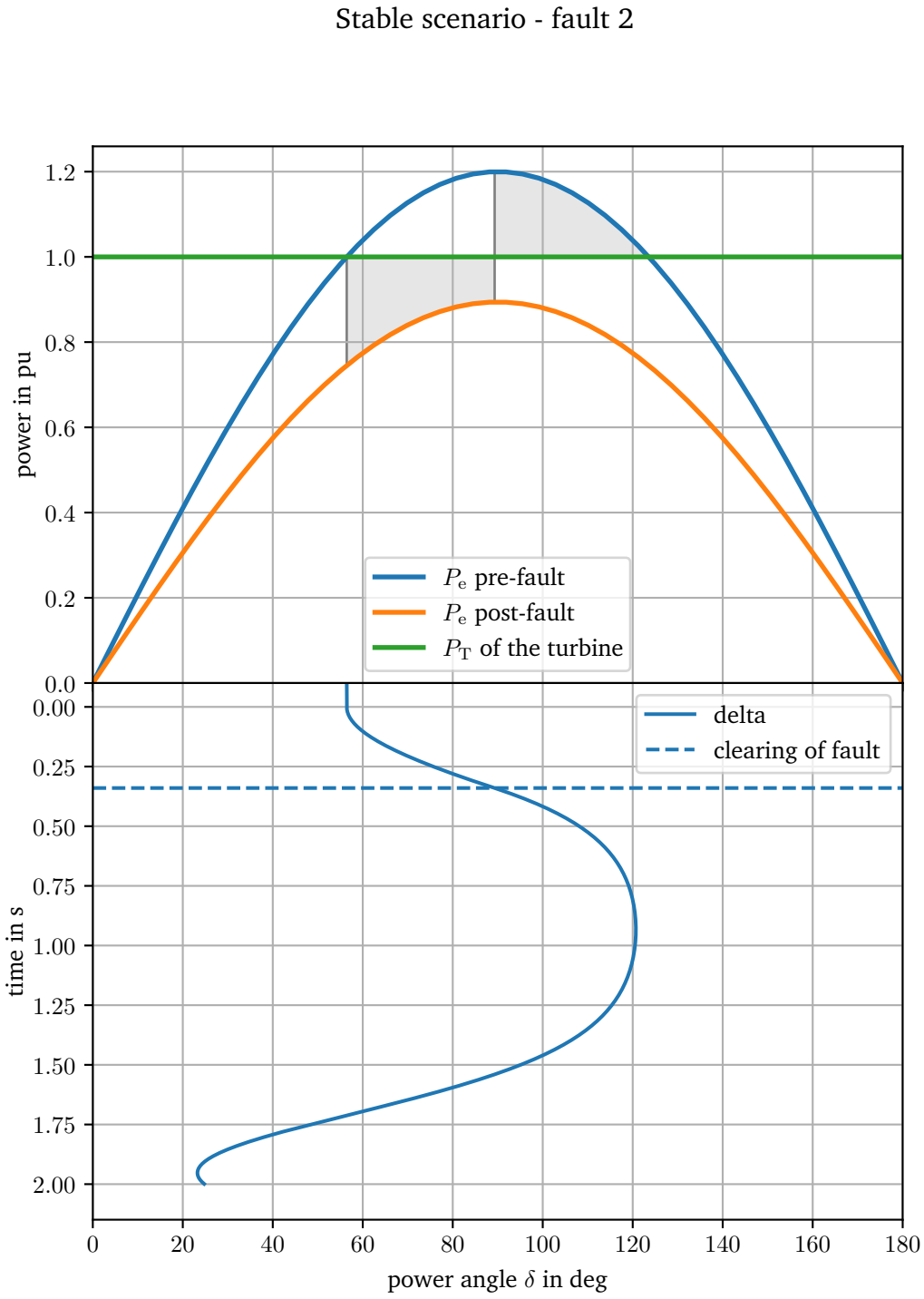
Stable scenario - fault 2
power in pu
1.2
1.0
0.8
0.6
0.4
0.2
0.0
P_e pre-fault
P_e post-fault
P_T of the turbine
time in s
0.00
0.25
0.50
0.75
1.00
1.25
1.50
1.75
2.00
delta
clearing of fault
0
20
40
60
80
100
120
140
160
180
power angle δ in deg

h

Unstable scenario - fault 2

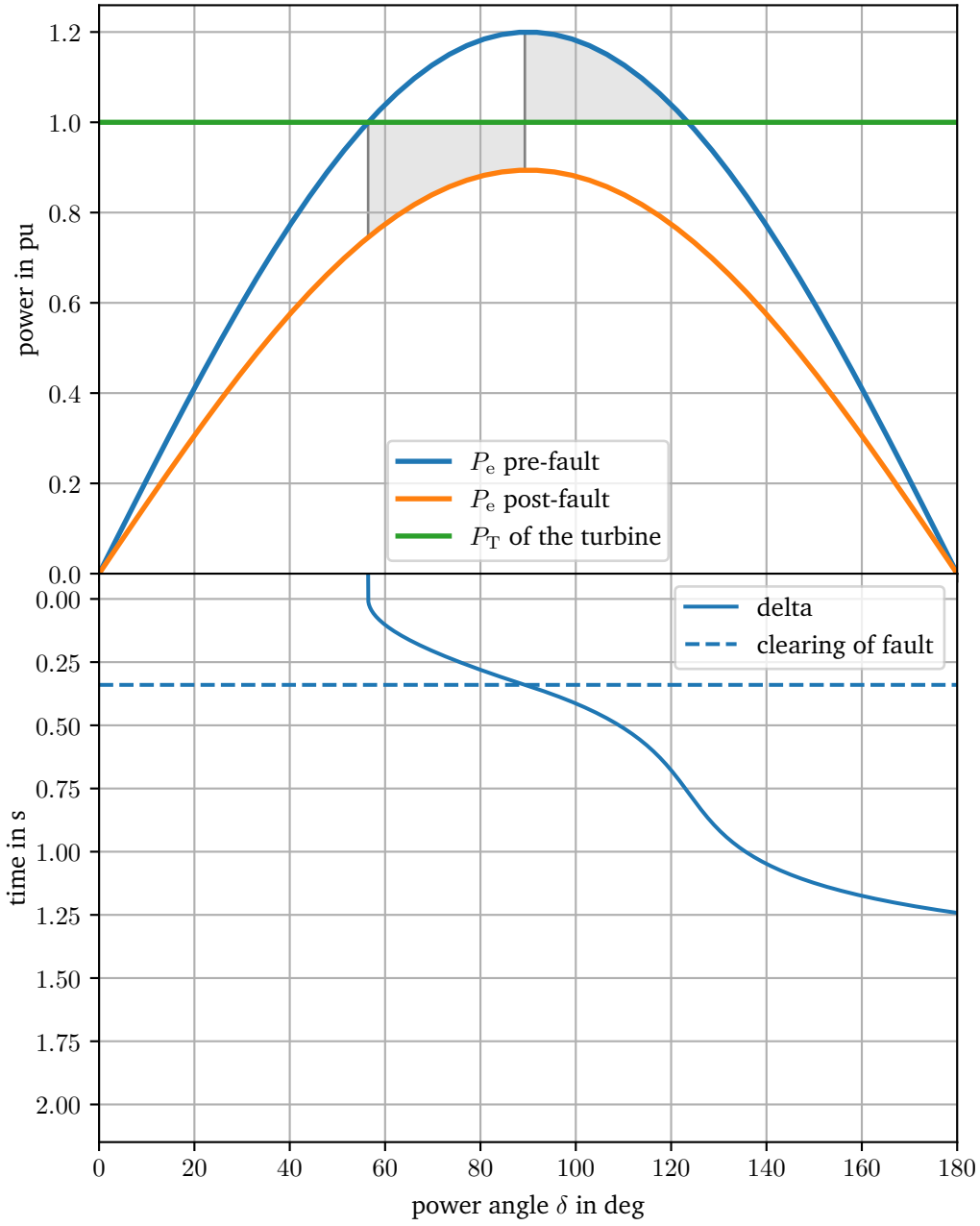

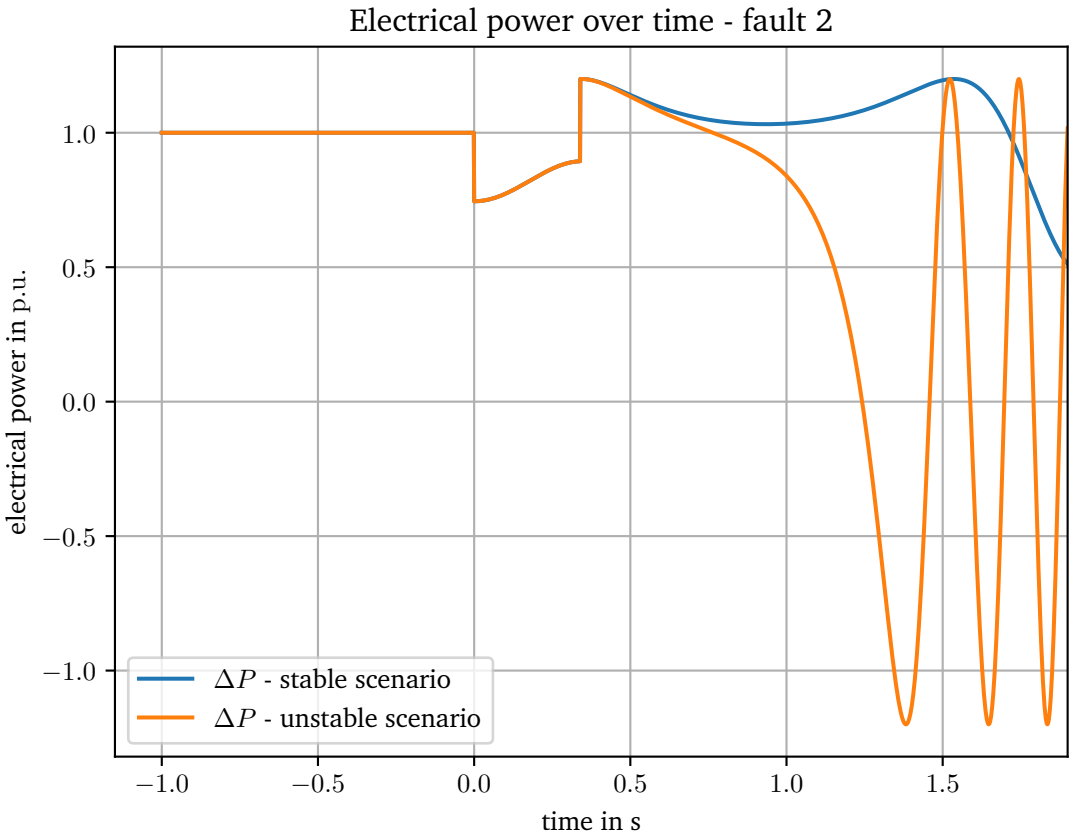
Electrical power over time - fault 2
electrical power in p.u.
time in s
1.0
0.5
0.0
−0.5
−1.0
−1.0
−0.5
0.0
0.5
1.0
1.5
ΔP - stable scenario
ΔP - unstable scenario

j

A.4 Fault 3

Stable scenario - fault 3

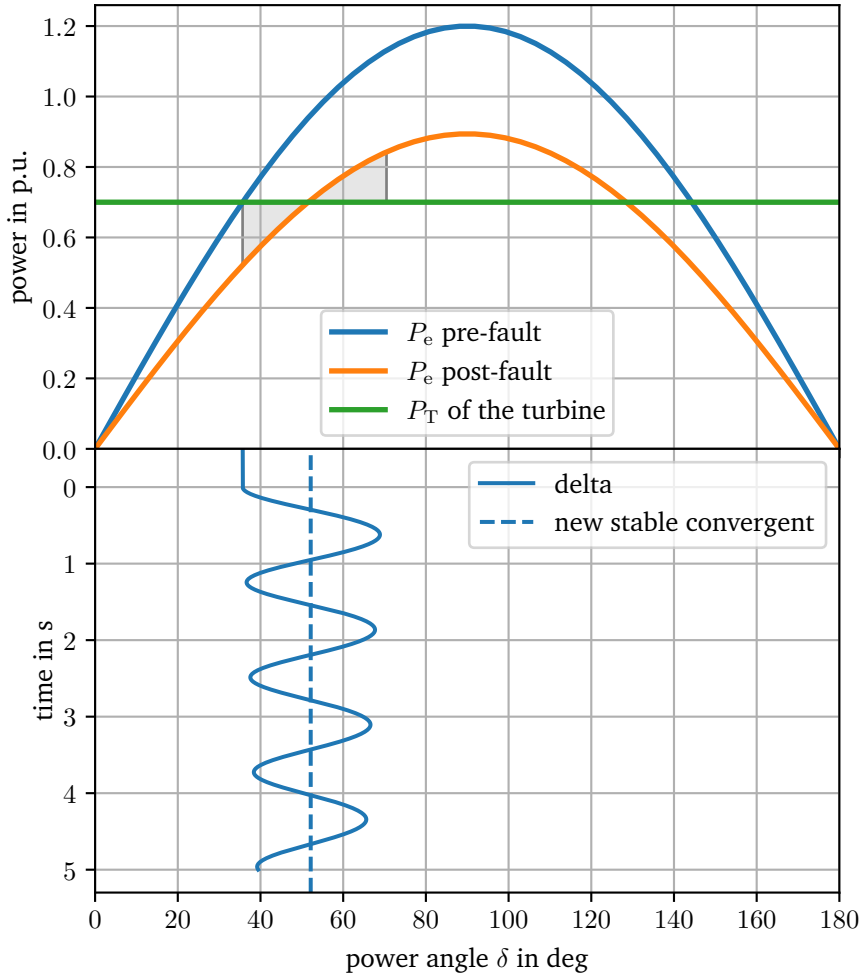

k

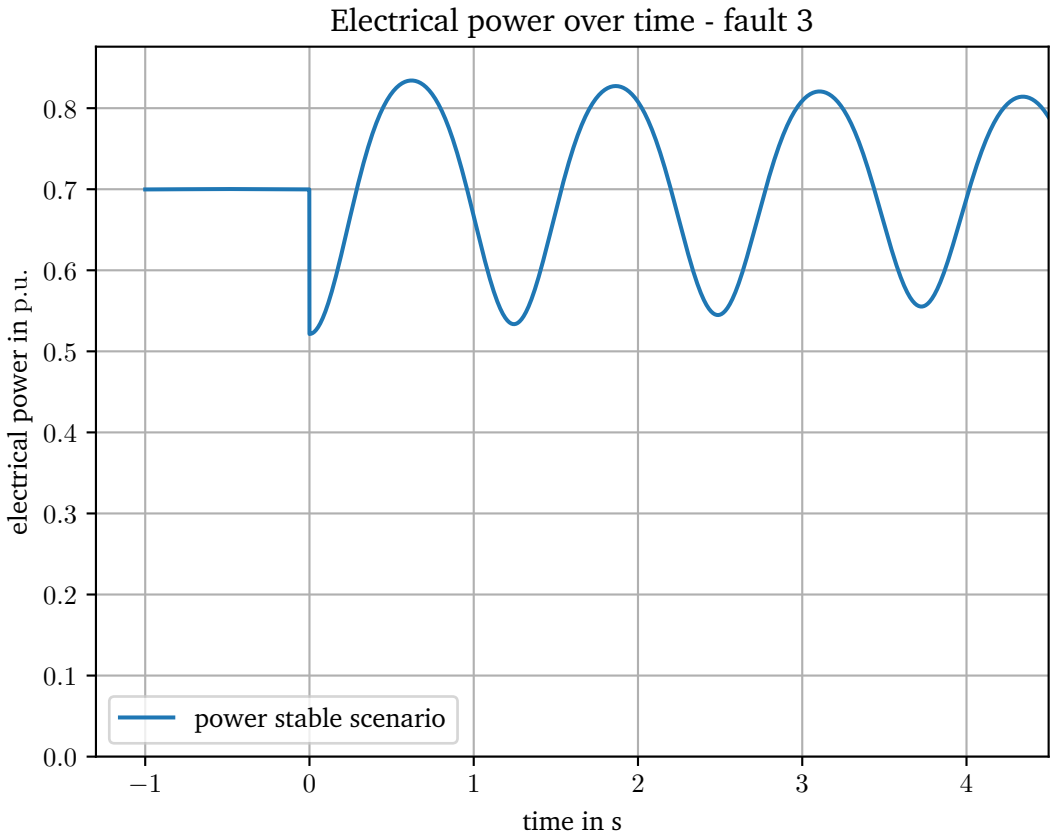
Electrical power over time - fault 3
electrical power in p.u.
time in s
power stable scenario
0.0
0.1
0.2
0.3
0.4
0.5
0.6
0.7
0.8
−1
0
1
2
3
4

A.5 Comparison algebraic vs. non-algebraic

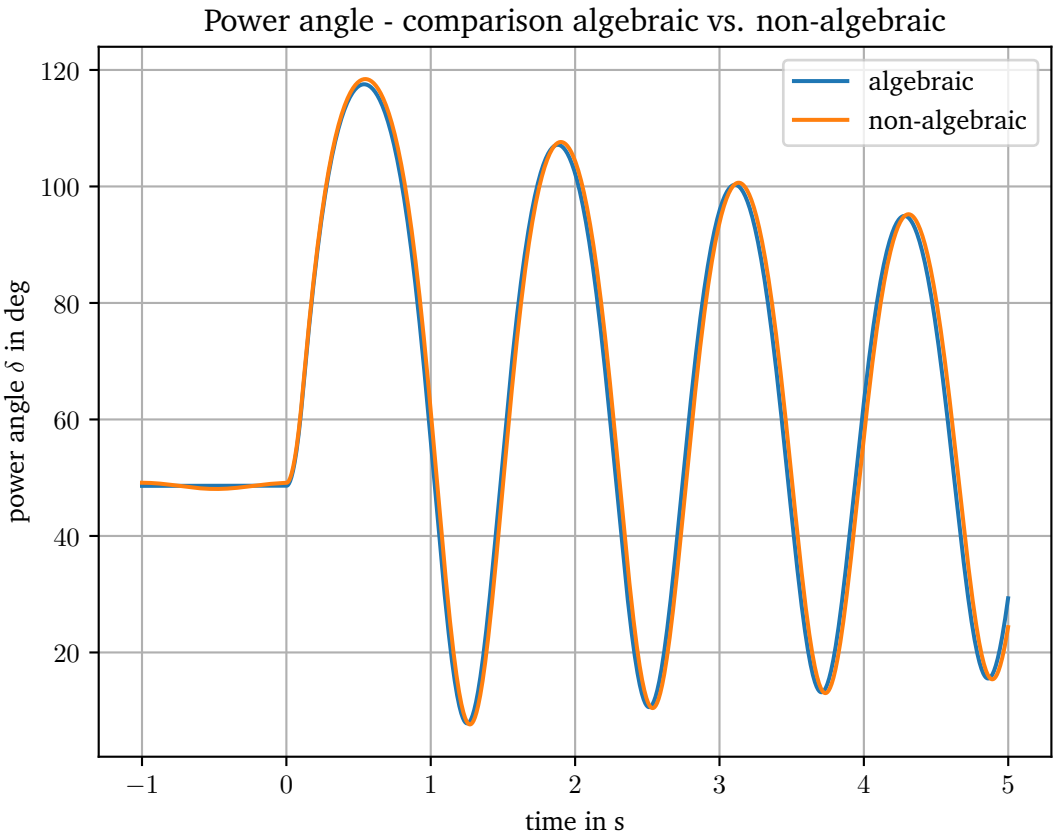

m

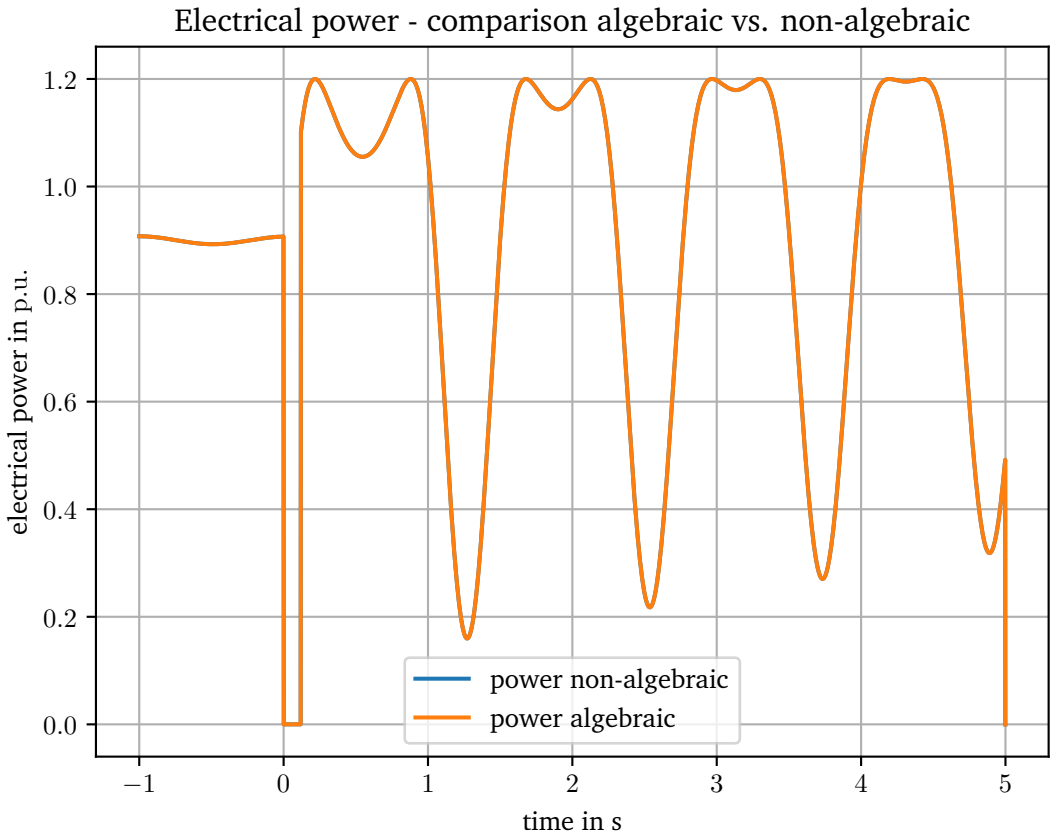
Electrical power - comparison algebraic vs. non-algebraic
electrical power in p.u.
time in s
power non-algebraic
power algebraic
1.2
1.0
0.8
0.6
0.4
0.2
0.0
−1
0
1
2
3
4
5

n